8—38
High Performance 3D Sensors for the characterization of Road Surface Defects

John Laurent[1]
Industrial Vision and 3D Sensors
INO

Jean-François Hébert [2]
Industrial Vision and 3D Sensors
INO

Abstract

Two different optical configurations were developed and are described. The first is a laser profiling system that is used for transverse profile acquisition for rut detection purposes. The second uses an auto-synchronized laser scanning sensor for crack detection Both these systems have been installed on inspection vehicles and have been tested. Tests have shown results that have a very good correlation with the current manual measurement methods for both ruts and cracks.

1   Laser Rut Measurement System

The LRMS is a transverse profiling system that detects and characterizes pavement rutting. It can acquire 4-metre wide profiles of a highway lane at normal traffic speeds. The system uses two laser profilers that digitize transverse sections of the road pavement. Custom optics and high-power laser line projectors allow the system to operate in daylight or in night-time as well as under varying pavement conditions. Road transverse profile data is collected and processed in real time on board the vehicle. Data filtering and rut extraction algorithms have been developed to automatically measure rut depth and rut width.

The main hardware components of the LRMS are the two triangulation-based laser line profilers. These components are responsible for the measurement of the left and right side transverse profiles. The laser profilers are mounted side-by-side on the back of the inspection vehicle (see figure 1).
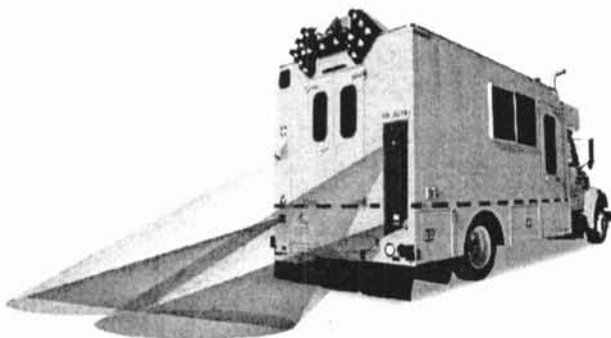

Figure 1: LRMS system installed on a Quebec Ministry of Transportation vehicle.

The LRMS specifications are given in the following table:

Nbr. of laser profilers	2
Sampling rate (max.)	25 profiles/s
Vehicle speed	0 to 120 km/h
Profile spacing	Adjustable
Transverse resolution	1280 points
Transverse field-of-view	4 m
Depth range of operation	500 mm
Z-axis (depth) accuracy	±1 mm
X-axis (transverse) accuracy	±3 mm

Table 1: LRMS Specifications

When rutting is measured manually a rigid steel rod typically of 1.6m to 1.8m long is laid across the road and the maximum distance between the pavement and the rod is taken as the rut depth. The rut analysis algorithm we developed mimics this process and has been written to conform to the ASTM E1703 norm for manual rut bar measurements. The rut depth information can be calculated in real time on board the vehicle or offline after all the road profile data has been gathered. The algorithm is implemented in four steps: filtering and linear approximation of the profile, search for rut support points and finally measurement of the rut depth/width as shown in figure 2.
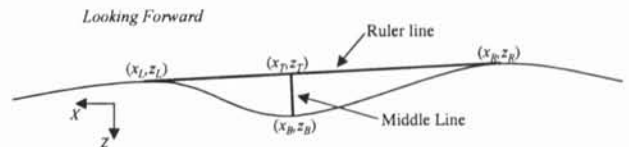

Figure 2: Manual rut

$$\text{Rut Depth} = \text{sqrt} \{ (x_B - x_T)^2 + (z_B - z_T)^2 \}$$
$$\text{Rut Width} = \text{sqrt} \{ (x_R - x_L)^2 + (z_R - z_L)^2 \}$$

To ensure that the LRMS produces measurements that are precise (in terms of repeatability) and unbiased, the system was tested by the MTQ (Quebec Ministry of Transportation). The MTQ subjected the LRMS to rut depth measurement validation tests on paths presenting varied deterioration conditions. Twelve 400m paths were selected, allowing the assessment of 48 segments of 100 m each. The rut depth was measured manually with a 1.8 m beam every 10 m and the mean of the ten readings was computed to obtain a mean depth per 100 m. The LRMS system was then passed three times at 70km/h in two series of tests over each prepared path. The bias (mean deviation between the readings obtained by the LRMS

---
[1] Address: 2740, rue Einstein, Sainte-Foy, (Quebec) Canada G1P4S4. E-mail: john.laurent@ino.ca,

[2] Address: 2740, rue Einstein, Sainte-Foy, (Quebec) Canada G1P4S4 E-mail: jean-francois.hebert@ino.ca

system and the values obtained with the beam) and the coefficient of variation ((standard deviation/mean) x 100) were then computed.

As of spring 2002, the results obtained are presented in the following table:

	Path	Mean bias 100 m segment (mm)	% bias less than 3 mm	Mean C.V. for a day	Mean C.V. for two days
	Left	0.4	100.0%	6.0%	
Day 1	Right	-0.3	98.0%	7.5%	
	mean	0.0	100.0%	4.6%	
	Left	0.5	100.0%	4.6%	
Day 2	Right	-0.6	95.8%	6.4%	
	mean	-0.1	100.0%	3.8%	
	Left	0.4	100.0%	5.3%	6.2%
Both days	Right	-0.4	96.9%	7.0%	8.4%
	mean	-0.0	100.0%	4.2%	5.2%

Table 2 : Result of road tests of the LRMS system.

Table 2 illustrates that for each of the tests the mean bias between the manual and LRMS rut measurements bias over a 100m segment was always less than 1mm. Furthermore, the bias always varied by less than 3mm for all the tests over 95% of the time.

2 Laser Crack Detection System (LCDS)

A second system based on a different optical configuration (auto-synchronized laser scanning) was also developed for the purpose of high-speed crack detection.

Figure 3 : Photo of the LCDS on the inspection vehicle.

The use of the auto-synchronized laser scanning technique allows for a much improved lateral resolution and a higher sampling rate as compared to the LRMS system. For the LCDS system two laser scanners are placed at the rear of the inspection vehicle 2m apart and 2m above the road surface which allows the system to see full 4m wide road lanes without having the sensors extend past the normal vehicle's width (see figure 3).

The following table summarizes the specifications of the LCDS system.

Nbr. of laser profilers	2
Sampling rate (max.)	300 profiles/s
Vehicle speed	0 to 70 km/h
Profile spacing	Adjustable
Transverse resolution	2048 points
Transverse field-of-view	4 m
Depth range of operation	500 mm
Z-axis (depth) accuracy	± 0.3 mm
X-axis (transverse) accuracy	± 2 mm

Table 3: LCDS Specifications

The two laser scanners are each capable of acquiring 1024 points per scan at a maximum scan rate of 300 profiles per second. Each sensor has a 60 degree field of view and a 0.5 m depth of field. The position detector used is a 128 pixel line array. Sub-pixel analysis is used in order to position the spot position to around 1/10 of a pixel. Figure 4 below illustrates the optical principal of the sensor.
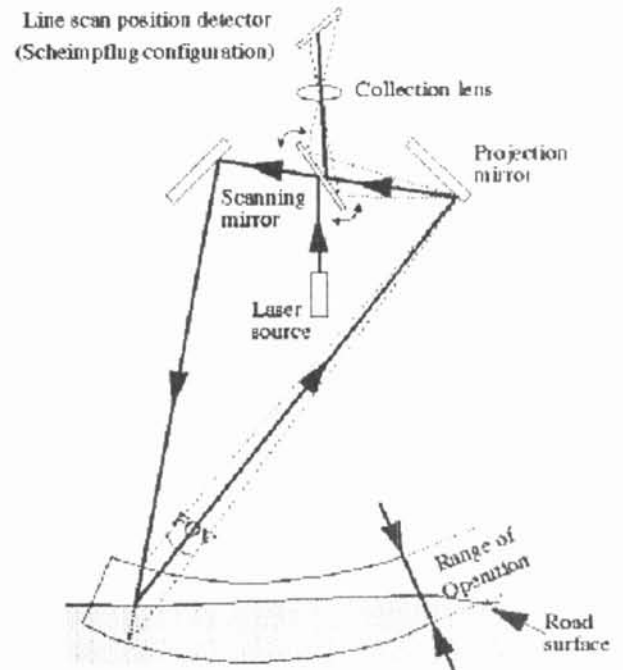

Figure 4: Auto-synchronized laser scanning principle.

The sensor is also composed of a high power laser point source and a galvanometer with a two sided mirror that is used to scan the laser spot over the road surface. The collection optics is automatically oriented towards the spot by the second side of the scanning mirror. This technique allows the use of high focal length (200mm)

collection lens which gives the sensor unmatched vertical precision. An interference filter placed in front of the collection lens allows the sensor to be insensitive to the outside lighting conditions so that the system can operate in both daytime and at night.

Crack detection algorithms were also developed in order to extract crack maps from the raw 3D data. The algorithm developed was implemented in two steps. The first step is the valley detection of candidate cracks in individual road profiles. The second step is the crack following and validation algorithm.

The valley detection algorithm in its present form is simply an exhaustive search for crack sized holes with minimum and maximum size constraints which are manually set by the operator depending on the asphalt texture and severity of the cracking conditions.
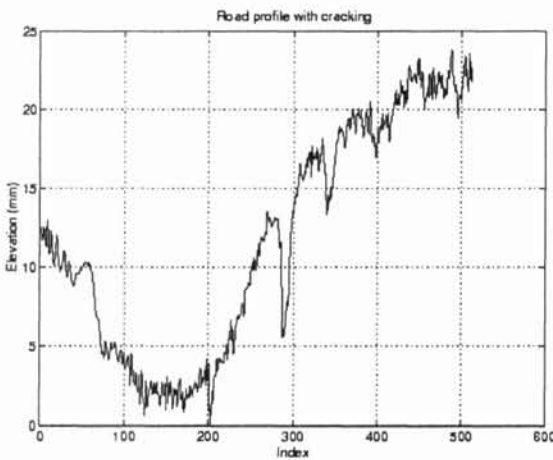

Figure 5 : Example 3D road profile with cracks.

For each 3 cm segment of 3D road profile, a hole detection and validation process is attempted. In this process, the minimal elevation point of the initial segment is used as the central point of a new 3 cm segment. The points 1.5 cm to either side of the central point are then analyzed to find the maximum elevation points on both sides. The hole depth is then measured as the difference between the low and average of the two high elevation points. The hole width is taken as the distance between the two maximum elevation points. If the hole depth is greater than a minimum threshold and the width is smaller than a maximum threshold than the hole is marked as a potential crack segment by the valley detection algorithm. The process then repeats for the next 3 cm segment offset 1.5 cm from the last central point. This technique is fast and easy to implement, yet it avoids getting caught in local minima.

The second step is the crack following and validation algorithm. After all the profiles have been analyzed by the valley detection algorithm, the result is a series of points which have been marked on the various profiles as potential crack segment candidates. These points are then analyzed by the crack following and validation algorithm in order to eliminate many of the spurious detections and to produce a crack map. This algorithm starts by searching the neighborhood of each potential crack

segment for the presence of other supporting points. The closest neighboring point is then identified. If this point is closer than a maximum distance threshold the process is than repeated recursively with the new point. If a string of several points can thus be aligned then they are validated as a crack and are connected with straight line segments to form part of the crack map.

As a indicative test of the crack detection algorithms several 400 m segments of roads with natural cracks were also scanned. The results of one such segment are presented here.
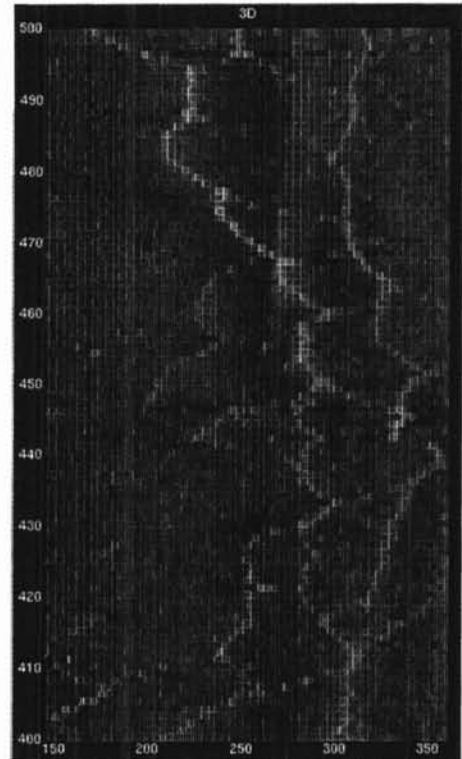

Figure 6 : Range image of road segment with the presence of alligator cracking.
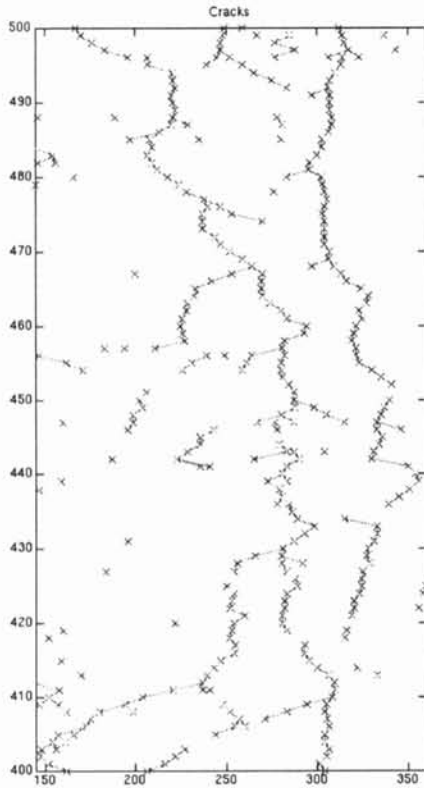
Figure 7: Extraction results of the crack detection algorithm (x's are the results of the valley detection).

In order to characterize the performance of the LCDS (in terms of performance and repeatability) the system was tested in collaboration with the MTQ. Because of the difficulty in manually measuring real cracks, an artificial crack test track was built. This track was created by manually cutting crack patterns of variable width, depth, orientation and length on two new 400m asphalt sections with a saw (see figure 8). With such a test track it was possible to know exactly what the length, depth and width of each crack was and thus it was possible to analyze the crack detection results of the LCDS.

Figure 8 : Photo of the test track on which artificial cracks were manually created using a saw.

The LCDS system was then passed nine times in two series of tests over each prepared path. All the tests were done at 70 km/h. Table 4 summarizes the results of the road tests on the artificial cracking test track.

Test criteria	Objectives	Results
Detection	80% of cracks >=3mm opening	98.6% of cracks
Length	Bias below 10% for each crack	Bias below 10% for 95% of all detected cracks
Opening (width)	± 4 mm for each crack	± 4 mm or better for 99.1% of detected cracks
Repeatability	Variation between any two passes < 0,05m/m2	Variation between any two passes < 0,028 m/m2

Table 4: Results of the LCDS of road tests conducted on the artificial cracking test track.

The results show very good detection results (over 98%) as well as low bias on the measurement of the length of the cracks (less than 10%). Severity (width) was also well measured (within specifications) over 99% of the time. Finally, the MTQ established goals for repeatability were beaten almost by a factor of two.

3   Conclusions

In this paper, two different optical configurations were described. The first is a laser profiling system that is used for transverse profile acquisition for rut detection purposes. The second uses an auto-synchronized laser scanning sensor for crack detection.

Comparison of the results from the laser rut measurement system with manual rut depth measurements shows that the mean bias over a 100m road segment is always less than 1mm. Furthermore, the bias always varied by less than 3 mm for all the tests over 95% of the time.

Because real crack data is difficult to measure and quantify, the laser crack detection system was characterized by scanning road segments with artificial crack patterns. Results show very good detection results (over 98%) as well as low bias on the measurement of the length of the cracks (less than 10%). Severity (width) was also well measured (within specifications) over 99% of the time. Finally, the MTQ established goals for repeatability were beaten almost by a factor of two.

References

[1] J. Laurent, M. Talbot, M. Doucet, "Road surface inspection using laser scanners for the high precision 3D measurements of large flat surfaces". Advances in 3D digital imaging and modeling, Ottawa, 1997

[2] J. Laurent, M. Talbot, M. Doucet, "Laser telemetry for the high precision 3D measurements of large flat surfaces". IAPR workshop on machine perception, Graz, Austria, 1996.

[3] F. Blais, M. Rioux, D. Gingras, J. Laurent "Three dimensional pavement inspection using a laser range sensor". Canadian electrical engineering and computer science congress, Quebec city, 1992